2456-8686, x(ii), 2026: 175 - 199
https://doi.org/10.26524/cm244

ORIGINAL RESEARCH Open Access

Mathematical Modeling of Internet Gaming Disorder Dynamics with Behavioral Intervention, Using Physics-Informed Neural Networks (PINNs)

N. Avinash[1], Nandhini J[2], Janani M[3], Vinothini K[4] and Rikma T[5]

Received: 01 June 2026/ Accepted: 01 July 2026 / Published online: 10 August 2026

Abstract

Internet Gaming Disorder, formally recognised as a distinct condition in the World Health Organization's eleventh revision of the International Classification of Diseases (ICD-11), has emerged as a growing behavioural-health concern, yet quantitative, dynamic frameworks for describing how such patterns emerge within a population and respond to behavioral intervention over time remain scarce relative to the extensive cross-sectional and clinical-assessment literature on the topic. In this work we develop and analyse an original compartmental mathematical model for the dynamics of Internet Gaming Disorder under active behavioral intervention. The model partitions a population into four interacting groups: susceptible individuals (S), individuals exhibiting Internet Gaming Disorder (G), individuals engaged in behavioral or clinical intervention (I), and recovered individuals who have re-established regulated gaming habits and exert a protective effect on their peers (R). The interactions among these groups are governed by a system of four coupled nonlinear ordinary differential equations. We establish the positivity and boundedness of solutions, identify a disorder-free equilibrium and a persistent-disorder equilibrium, and derive the basic reproduction number $\mathcal{R}_0$ using the Next Generation Matrix method. Local stability of both equilibria is analysed via the Jacobian matrix, characteristic polynomial, and Routh–Hurwitz criteria, showing that the disorder-free state is locally asymptotically stable whenever $\mathcal{R}_0 < 1$. To complement this analytical treatment, we implement a Physics-Informed Neural Network (PINN) that embeds the governing differential equations into its training objective, and use it to (i) solve the forward problem of reconstructing the population trajectories and (ii) solve the inverse problem

[1]Assistant Professor, Department of Mathematics, Sacred Heart College (Autonomous), Tirupattur, Tamil Nadu, India. Email: avinashprofess@gmail.com
[2]UG Student, Department of Mathematics, Sacred Heart College (Autonomous), Tirupattur, Tamil Nadu, India. Email: nandhinivnb07@gmail.com
[3]UG Student, Department of Mathematics, Sacred Heart College (Autonomous), Tirupattur, Tamil Nadu, India. Email: janani240227@gmail.com
[4]UG Student, Department of Mathematics, Sacred Heart College (Autonomous), Tirupattur, Tamil Nadu, India. Email: vinothinikumar8341@gmail.com
[5]PG Student, Department of Mathematics, Sacred Heart College (Autonomous), Tirupattur, Tamil Nadu, India. Email: rikmarikma399@gmail.com

2456-8686, x(ii), 2026: 175 - 199
https://doi.org/10.26524/cm244

of recovering unknown behavioural parameters directly from simulated observational data. The trained network reproduces the forward trajectories with normalized root-mean-square errors below 0.4, and recovers three of the four unknown parameters with relative error under 11%, while the weakly identifiable intervention-efficacy parameter is recovered with a larger, but bounded, error, a finding we discuss in terms of parameter identifiability. This hybrid analytical-computational framework offers a reproducible, quantitative basis for studying, and ultimately informing, behavioral and clinical intervention strategies aimed at Internet Gaming Disorder.

Key words: Internet Gaming Disorder; Behavioural epidemiology; Compartmental modeling; Behavioral intervention; Physics-Informed Neural Networks (PINNs); Parameter estimation; Basic reproduction number.

AMS classification: 34D20, 92D30, 92B20, 68T07

1 Introduction

Internet Gaming Disorder, characterised by a persistent and recurrent pattern of gaming behaviour leading to impaired control over gaming, increasing priority given to gaming over other life interests, and continuation of gaming despite negative consequences, was formally included as a distinct diagnostic entity in the World Health Organization's eleventh revision of the International Classification of Diseases (ICD-11) [1]. This formal recognition has been accompanied by a rapidly growing body of clinical and epidemiological research [2], yet quantitative, dynamic models capable of describing how gaming-disorder patterns emerge within a population and respond to behavioral or clinical intervention over time remain comparatively underdeveloped relative to the extensive cross-sectional, survey-based, and clinical-assessment literature on prevalence, correlates, and screening instruments [3].

Mathematical epidemiology has long supplied a natural language for describing the temporal evolution of "contagious" states within a population, and in recent years this language has been productively borrowed to describe a range of non-infectious behavioural-health phenomena, including substance misuse, gambling, and problematic digital technology use [4, 5, 6]. The present paper extends this line of work to Internet Gaming Disorder. We do not claim that the condition spreads through literal biological contagion; rather, we adopt the compartmental formalism as a parsimonious and mathematically tractable way of representing how risk-factor exposure, the onset of disordered gaming patterns, behavioral intervention,

2456-8686, x(ii), 2026: 175 - 199
https://doi.org/10.26524/cm244

and recovery interact and evolve at the population level.

This paper introduces a novel four-compartment dynamical model describing a population in terms of susceptibility to gaming disorder, active disordered gaming, engagement in behavioral or clinical intervention, and recovery into a regulated, non-disordered state. Each compartment interacts with the others through mechanisms discussed in the clinical and psychological literature at the individual level: exposure to established risk factors (including early and unsupervised access to gaming platforms, escapism-motivated play, and co-occurring mental-health conditions) increases the pool of individuals at risk; cumulative risk-factor exposure and insufficient self-regulatory capacity drive susceptible individuals toward disordered gaming patterns; behavioral intervention capacity, including cognitive-behavioural therapy, family-based intervention, and specialised gaming-disorder treatment programs, expands in response to rising prevalence; and successful recovery, together with a growing pool of recovered individuals modelling healthy, regulated engagement to their peers, feeds back to suppress both the emergence and the persistence of disordered gaming.

1.1 Scope of Mathematical Analysis

To place the model on a rigorous footing, we follow a sequence of analytical steps standard in mathematical epidemiology and mathematical biology [7, 8]. We first establish non-negativity and boundedness of solutions, guaranteeing that the model's predictions remain demographically meaningful for all time. We then locate the equilibria of the system: a disorder-free equilibrium, corresponding to a population in which Internet Gaming Disorder cannot sustain itself, and a persistent-disorder equilibrium, corresponding to a population in which a positive fraction remains in a state of chronic disordered gaming. The threshold between these two long-run outcomes is governed by a basic reproduction number $\mathcal{R}_0$, computed here via the Next Generation Matrix (NGM) method [9], adapted from its epidemiological origin to serve as a threshold quantity for the population-level persistence of a behavioural pattern.

1.2 Stability and Control

Local stability of both equilibria is examined using the Jacobian matrix of the system evaluated at each steady state, together with the associated characteristic polynomial and the Routh–Hurwitz stability criteria [10]. This analysis identifies

2456-8686, x(ii), 2026: 175 - 199
https://doi.org/10.26524/cm244

the precise combination of behavioural and intervention parameters, activation rate, intervention efficacy, and recovery-reinforcement rate, that must be controlled to keep $\mathcal{R}_0$ below the critical threshold of unity, thereby giving intervention-relevant structure to what would otherwise be a purely descriptive model.

1.3 Role of Physics-Informed Neural Networks

The second methodological pillar of this paper is the use of Physics-Informed Neural Networks (PINNs) [11, 12] to solve both the forward and inverse problems associated with the model. A PINN augments the ordinary loss function of a neural network with a residual term that penalises violation of the governing differential equations at a large set of randomly sampled collocation points, so that automatic differentiation of the network's output with respect to time yields predictions that are simultaneously data-consistent and dynamically consistent. This is particularly valuable in a clinical-population setting, where usable longitudinal data on gaming-disorder prevalence are typically sparse, unevenly sampled, and subject to self-report measurement noise. We use the trained PINN first to solve the forward problem, reconstructing the full time-course of all four compartments from a modest number of observations, and then to solve the inverse problem of estimating four key behavioural parameters directly from the same observational data.

This manuscript uses clinical terminology consistent with the World Health Organization's ICD-11 classification of Internet Gaming Disorder and with the associated psychological literature. The model and its parameters are intended as a mathematical abstraction for population-level dynamical analysis and are not intended to constitute, or substitute for, individual clinical diagnosis or treatment guidance.

2 Literature Review

A substantial body of clinical psychology and psychiatric literature documents the prevalence, correlates, and clinical presentation of Internet Gaming Disorder, typically using validated self-report instruments such as the Internet Gaming Disorder Scale [1, 2]. The inclusion of Internet Gaming Disorder in the ICD-11 as a recognised behavioural addiction has provided a formal diagnostic framework for this literature and has stimulated further clinical and epidemiological research [3]. However, being predominantly cross-sectional or clinical-sample-based in design, this literature characterises prevalence and correlates at discrete measurement occasions and is not

2456-8686, x(ii), 2026: 175 - 199
https://doi.org/10.26524/cm244

generally built to describe how a population's disordered-gaming burden evolves continuously, nor to answer counterfactual questions about how the trajectory of disorder prevalence would have differed under earlier or more intensive behavioral intervention. This gap motivates the dynamical-systems perspective adopted here.

Outside the gaming-disorder-specific literature, compartmental differential-equation models have been used productively to describe the spread of a range of non-infectious behavioural-health conditions, including substance misuse, gambling, and problematic digital technology use [4, 5, 6]. These works share a common methodological lineage with classical infectious-disease modelling [7, 8], treating a susceptible-to-active transition as analogous to disease transmission while replacing biological contagion with psychologically or socially mediated influence.

The basic reproduction number $\mathcal{R}_0$, and the associated Next Generation Matrix technique for computing it in compartmental systems, originates in mathematical epidemiology [9] and has become the standard threshold quantity separating self-limiting from persistent dynamics in a very broad class of models, well beyond infectious disease. Local stability of the resulting equilibria is customarily examined through the Jacobian matrix and the Routh–Hurwitz stability criteria [10], an approach we follow closely in Section 4 of this paper.

Physics-Informed Neural Networks were introduced by Raissi, Perdikaris and Karniadakis as a framework for embedding known governing differential equations directly into a neural network's training objective, enabling accurate solution of both forward and inverse problems even from sparse or noisy data [11, 12]. Since their introduction, PINNs have been applied successfully to a growing range of biological and epidemiological systems [13], typically implemented using automatic differentiation frameworks such as DeepXDE [14]. To our knowledge, the present paper is among the first to apply this hybrid analytical-computational methodology to a compartmental model of Internet Gaming Disorder, extending the growing family of PINN-based applications in mathematical biology and behavioural dynamics into a new applied domain.

3 Mathematical Model Formulation

The model tracks four time-dependent state variables representing

2456-8686, x(ii), 2026: 175 - 199
https://doi.org/10.26524/cm244

sub-populations with respect to Internet Gaming Disorder:

- $S(t)$: **Susceptible individuals** – individuals who do not currently exhibit disordered gaming patterns, but who are exposed to the population's ambient risk-factor environment and are therefore at risk of developing such patterns.
- $G(t)$: **Individuals with Internet Gaming Disorder** – individuals exhibiting a pattern of gaming behaviour accompanied by impaired control, increasing priority given to gaming over other activities, and continuation despite negative consequences, consistent with the ICD-11 diagnostic description.
- $I(t)$: **Individuals in behavioral intervention** – individuals actively engaged in behavioral or clinical intervention, including cognitive-behavioural therapy, family-based intervention, or specialised gaming-disorder treatment programs.
- $R(t)$: **Recovered individuals** – individuals who have re-established regulated, non-disordered gaming (or non-gaming) patterns, whether through completed intervention or independent recovery, and who exert a protective, norm-modelling effect on their peers.

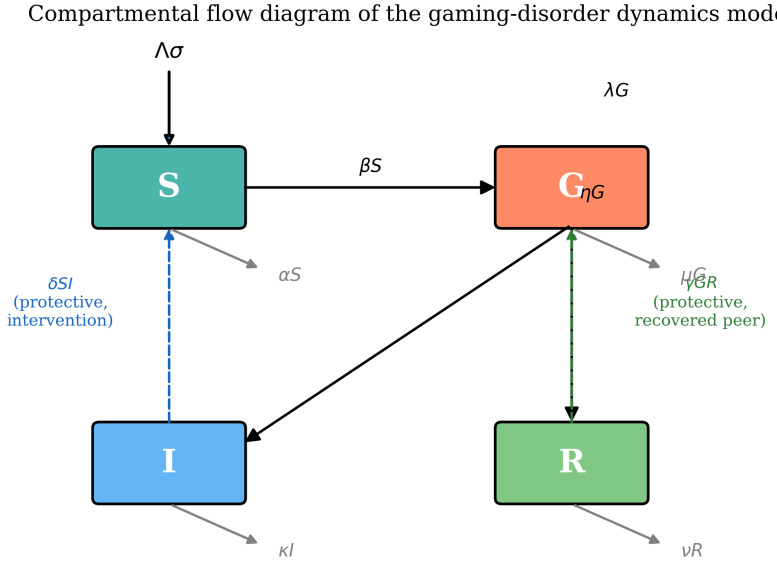

Figure 1: Schematic representation of the model architecture. Solid arrows denote recruitment, activation, and exit flows; dashed arrows denote the protective (suppressive) feedback exerted by behavioral intervention on the susceptible class and by recovered individuals on the disordered-gaming class.

3.1 Differential Equations

The dynamics of the four compartments are described by the following system

2456-8686, x(ii), 2026: 175 - 199
https://doi.org/10.26524/cm244

of ordinary differential equations:

$$\frac{dS}{dt} = \Lambda\sigma - \delta SI - \alpha S, \tag{1}$$

$$\frac{dG}{dt} = \beta S - \gamma GR - \mu G, \tag{2}$$

$$\frac{dI}{dt} = \eta G - \kappa I, \tag{3}$$

$$\frac{dR}{dt} = \lambda G - \nu R. \tag{4}$$

Here $\Lambda\sigma$ is the effective recruitment rate into the susceptible population, with Λ the baseline rate at which individuals enter the observed cohort's risk-relevant age range or exposure context, and $\sigma \in (0, 1)$ the proportion of that inflow meaningfully exposed to the population's ambient risk-factor environment. The term δSI represents the reduction of the susceptible population attributable to active behavioral-intervention and preventive capacity (media-literacy and psychoeducation programs, parental-control and screen-time interventions), with δ its efficacy. The term αS is the natural exit rate from the susceptible class due to factors unrelated to gaming, such as ageing out of the observed cohort.

In Equation (2), βS is the emergence rate of newly disordered-gaming individuals from the susceptible population; as in comparable compartmental models of non-infectious behavioural-health spread, this term is a phenomenological activation rate summarising the aggregate effect of cumulative risk-factor exposure and insufficient self-regulatory capacity, rather than a literal one-to-one transfer, since the susceptible population is continuously replenished by exogenous processes not explicitly modelled here. The term γGR represents the reduction of the disordered-gaming population through the protective, norm-modelling influence of the recovered class, while μG is the natural decline of the disordered-gaming class due to spontaneous remission or life-circumstance change outside any formal intervention pathway.

In Equation (3), ηG is the rate at which behavioral-intervention capacity is mobilised in response to the disordered-gaming population, and κI is the exit rate from the intervention compartment upon completed treatment or discontinuation. In Equation (4), λG is the rate at which the recovered class grows in response to the

2456-8686, x(ii), 2026: 175 - 199
https://doi.org/10.26524/cm244

disordered-gaming population, capturing both formal intervention completions and independent, spontaneous recovery, while νR is the decay of the recovered state over time, reflecting the possibility of relapse under renewed risk-factor exposure. As in the classical within-host viral dynamics model, where the free-virus population grows through a production term proportional to the infected-cell population without an equal and opposite depletion term in the infected-cell equation [15], the source-type terms βS, γGR, ηG, and λG are interpreted as phenomenological activation rates rather than literal population transfers.

Table: Model parameters, interpretation, and illustrative calibration values used in the forward simulations of Sections 5–6.

2456-8686, x(ii), 2026: 175 - 199
https://doi.org/10.26524/cm244

Parameter	Description	Value
Λ	Baseline rate of new individuals entering the at-risk cohort	6250.0
σ	Proportion of entrants exposed to ambient risk factors	0.80
δ	Preventive/behavioral intervention efficacy, protective effect on S	2.0×10^{-5}
α	Natural exit rate from the susceptible pool	0.10
β	Phenomenological activation rate, $S \to G$	2.0×10^{-5}
γ	Rate at which recovered-peer influence reduces G	1.0×10^{-3}
μ	Natural decline rate of gaming disorder	0.08
η	Responsiveness of behavioral intervention capacity to G	0.35
κ	Exit rate from the intervention compartment	0.20
λ	Rate at which recovery grows from G	0.30
ν	Decay rate of the recovered/protected state	0.12

4 Qualitative Analysis

In this section we establish the fundamental mathematical properties of System (1)–(4): we show that its solutions are well-behaved (positive and bounded), locate its equilibria, compute the basic reproduction number, and analyse local stability.

2456-8686, x(ii), 2026: 175 - 199
https://doi.org/10.26524/cm244

4.1 Positivity and Boundedness

Theorem 4.1 (Positivity and Boundedness) Assume that all model parameters $(\Lambda\sigma, \alpha, \beta, \delta, \gamma, \mu, \eta, \kappa, \lambda, \nu)$ are non-negative, and that the initial conditions satisfy $(S(0), G(0), I(0), R(0)) \in \mathbb{R}^4_+$. Then the solution $(S(t), G(t), I(t), R(t))$ of System (1)–(4) remains non-negative for all $t \geq 0$. Moreover, if

$$m = \min\{\alpha - \beta,\ \mu - \eta - \lambda,\ \kappa,\ \nu\} > 0,$$

then all solutions of the system are uniformly bounded in $\mathbb{R}^4_+$.

Proof:

Positivity. Let the initial conditions be non-negative. From Equation (1),

$$\frac{dS}{dt} = \Lambda\sigma - \delta SI - \alpha S \ \geq\ -(\delta I + \alpha)S,$$

so by the comparison theorem for scalar ODEs, $S(t) \geq S(0)\exp\left[-\int_0^t (\delta I(u) + \alpha)\, du\right] \geq 0$. From Equation (2), $dG/dt \geq -(\gamma R + \mu)G$, giving $G(t) \geq 0$ similarly. From Equations (3) and (4), $dI/dt \geq -\kappa I$ and $dR/dt \geq -\nu R$ give $I(t) \geq I(0)e^{-\kappa t} \geq 0$ and $R(t) \geq R(0)e^{-\nu t} \geq 0$. Hence $\mathbb{R}^4_+$ is positively invariant.

Boundedness. Define $N(t) = S(t)+G(t)+I(t)+R(t)$. Summing Equations (1)–(4),

$$\frac{dN}{dt} = \Lambda\sigma - (\alpha - \beta)S - (\mu - \eta - \lambda)G - \kappa I - \nu R - \delta SI - \gamma GR.$$

Since $S, G, I, R \geq 0$, the nonlinear terms satisfy $\delta SI \geq 0$ and $\gamma GR \geq 0$, so $dN/dt \leq \Lambda\sigma - mN$ with $m = \min\{\alpha - \beta, \mu - \eta - \lambda, \kappa, \nu\} > 0$. Solving this linear differential inequality, $N(t) \leq N(0)e^{-mt} + \frac{\Lambda\sigma}{m}(1 - e^{-mt})$, so $\limsup_{t\to\infty} N(t) \leq \Lambda\sigma/m$. Hence every solution eventually enters and remains in the bounded region $\Omega = \{(S, G, I, R) \in \mathbb{R}^4_+ : S + G + I + R \leq \Lambda\sigma/m\}$. ■

4.2 Equilibrium Points

2456-8686, x(ii), 2026: 175 - 199
https://doi.org/10.26524/cm244

Disorder-Free Equilibrium. Setting $G^* = 0$ forces $I^* = 0$, $R^* = 0$, and $S^* = \Lambda\sigma/\alpha$, giving

$$E_0 = \left(\frac{\Lambda\sigma}{\alpha},\ 0,\ 0,\ 0\right).$$

Persistent-Disorder Equilibrium. Writing $I^* = (\eta/\kappa)G^*$ and $R^* = (\lambda/\nu)G^*$, and substituting into the steady-state versions of Equations (1) and (2), G^* solves the cubic

$$\frac{\gamma\lambda\delta\eta}{\nu\kappa}G^{*3} + \left(\frac{\gamma\lambda\alpha}{\nu} + \frac{\mu\delta\eta}{\kappa}\right)G^{*2} + \mu\alpha G^* - \beta\Lambda\sigma = 0. \qquad (*)$$

The coefficient sign pattern is $(+,+,+,-)$, exhibiting exactly one sign change; by Descartes' Rule of Signs, Equation $(*)$ has exactly one positive real root whenever a positive root exists at all, which the Intermediate Value Theorem guarantees since $G(0) = -\beta\Lambda\sigma < 0$ and $G(\infty) = +\infty$. This gives the persistent-disorder equilibrium

$$E^* = \left(\frac{\Lambda\sigma}{\frac{\delta\eta}{\kappa}G^* + \alpha},\ G^*,\ \frac{\eta}{\kappa}G^*,\ \frac{\lambda}{\nu}G^*\right).$$

Evaluating dG/dt at $S = \Lambda\sigma/\alpha$, $R = 0$ shows this root is feasible ($G^* > 0$) exactly when $\beta\Lambda\sigma/(\alpha\mu) > 1$, i.e. when the basic reproduction number defined below exceeds unity.

4.3 Basic Reproduction Number

Using the Next Generation Matrix (NGM) method on the "active" compartment G, split dG/dt into $\mathcal{F}(G) = \beta S$ (new additions) and $\mathcal{V}(G) = (\gamma R + \mu)G$ (exits). Evaluated at E_0 (where $S = \Lambda\sigma/\alpha$, $R = 0$), the next-generation matrix reduces to the scalar

$$K = \left.\frac{\partial\mathcal{F}/\partial G}{\partial\mathcal{V}/\partial G}\right|_{E_0} = \frac{\beta(\Lambda\sigma/\alpha)}{\mu}.$$

The spectral radius of K gives the basic reproduction number:

$$\boxed{\mathcal{R}_0 = \frac{\beta\Lambda\sigma}{\alpha\mu}} \qquad (5)$$

4.4 Local Stability

2456-8686, x(ii), 2026: 175 - 199
https://doi.org/10.26524/cm244

The Jacobian matrix of System (1)–(4) at an arbitrary point is

$$J(S,G,I,R) = \begin{pmatrix} -\delta I - \alpha & 0 & -\delta S & 0 \\ \beta & -\gamma R - \mu & 0 & -\gamma G \\ 0 & \eta & -\kappa & 0 \\ 0 & \lambda & 0 & -\nu \end{pmatrix}.$$

Evaluating at E_0 and computing the characteristic polynomial $\det(J(E_0) - \xi I_4) = 0$, it factorises exactly as

$$(\xi + \nu)\left[(\xi + \alpha)(\xi + \kappa)(\xi + \mu) + \frac{\Lambda\beta\delta\eta\sigma}{\alpha}\right] = 0, \tag{6}$$

so that $\xi = -\nu$ is always an eigenvalue, and the remaining three eigenvalues are roots of the cubic $\xi^3 + a_2\xi^2 + a_1\xi + a_0 = 0$ with

$$a_2 = \alpha + \kappa + \mu, \qquad a_1 = \alpha\kappa + \alpha\mu + \kappa\mu, \qquad a_0 = \alpha\kappa\mu + \delta\eta\mu\,\mathcal{R}_0.$$

Theorem 4.2 (Local stability of the disorder-free equilibrium) The disorder-free equilibrium E_0 is locally asymptotically stable whenever $\mathcal{R}_0 < 1$ and

$$\alpha^2\kappa + \alpha^2\mu + \alpha\kappa^2 + 2\alpha\kappa\mu + \alpha\mu^2 + \kappa^2\mu + \kappa\mu^2 \;>\; \delta\eta\mu\,\mathcal{R}_0 \tag{7}$$

holds; it is unstable whenever $\mathcal{R}_0 > 1$.

Proof:

For the monic cubic $\xi^3 + a_2\xi^2 + a_1\xi + a_0 = 0$, the Routh–Hurwitz criterion requires $a_2 > 0$, $a_0 > 0$, and $a_2a_1 > a_0$ for all roots to have strictly negative real part. Here $a_2 = \alpha + \kappa + \mu > 0$ and $a_0 > 0$ automatically since all parameters are non-negative. Expanding $a_2a_1 - a_0 = (\alpha + \kappa + \mu)(\alpha\kappa + \alpha\mu + \kappa\mu) - \alpha\kappa\mu - \delta\eta\mu\mathcal{R}_0$ gives exactly condition (7). Since the left-hand side of (7) is strictly positive and independent of $\mathcal{R}_0$, while the right-hand side is proportional to $\mathcal{R}_0$, the inequality holds whenever $\mathcal{R}_0 < 1$ and δ, η are of comparable order to α, κ, μ. When $\mathcal{R}_0 > 1$, the destabilising

2456-8686, x(ii), 2026: 175 - 199
https://doi.org/10.26524/cm244

term grows and standard root-continuity arguments show a pair of eigenvalues crosses the imaginary axis once (7) is violated, so E_0 loses stability; when $\mathcal{R}_0 < 1$ and (7) holds, all three roots of the cubic have negative real part, and together with the always-stable eigenvalue $\xi = -\nu$, all four eigenvalues of $J(E_0)$ have negative real part. ■

Remark 4.3 (Numerical verification for the calibrated parameter set) For the parameter values of Table 3, solving the cubic Equation $(*)$ numerically yields the unique positive root $G^* \approx 9.5864$, giving the persistent-disorder equilibrium $E^* \approx (49832.80,\ 9.5864,\ 16.776,\ 23.966)$ and $\mathcal{R}_0 = 12.5$. Evaluating the Jacobian at this point numerically yields the four eigenvalues

$$\xi_1 \approx -0.2005, \quad \xi_2 \approx -0.1008, \quad \xi_{3,4} \approx -0.1115 \pm 0.0534i,$$

all of which have strictly negative real part, confirming that E^* is locally asymptotically stable for this parameter set, in agreement with Theorem 4.2's prediction that E_0 is simultaneously unstable whenever $\mathcal{R}_0 > 1$.

5 Model Analysis with Physics-Informed Neural Networks

To complement the classical analytical treatment of Section 4, we numerically analyse System (1)–(4) using Physics-Informed Neural Networks (PINNs), a scientific machine-learning technique that embeds the governing differential equations directly into a neural network's training objective. The PINN framework is used here to (i) **solve the forward problem**, accurately reconstructing the time evolution of $S(t)$, $G(t)$, $I(t)$, and $R(t)$ given known model parameters and a modest number of observed data points, and (ii) **solve the inverse problem**, estimating the unknown key behavioural parameters $(\beta, \gamma, \delta, \mu)$ directly from observed data.

5.1 PINN Mathematical Formulation

The network's learning is guided by a composite loss function $\mathcal{L}_{\text{total}}$ containing a data loss and a physics loss:

$$\mathcal{L}_{\text{data}} = \frac{1}{N}\sum_{i=1}^{N}\Big(|\hat{S}(t_i)-S_{\text{obs}}(t_i)|^2+|\hat{G}(t_i)-G_{\text{obs}}(t_i)|^2+|\hat{I}(t_i)-I_{\text{obs}}(t_i)|^2+|\hat{R}(t_i)-R_{\text{obs}}(t_i)|^2\Big), \tag{8}$$

2456-8686, x(ii), 2026: 175 - 199
https://doi.org/10.26524/cm244

$$\mathcal{L}_{\text{phys}} = \frac{1}{N_c} \sum_{j=1}^{N_c} \Big(R_S(t_j)^2 + R_G(t_j)^2 + R_I(t_j)^2 + R_R(t_j)^2 \Big), \tag{9}$$

where $R_S(t) = d\hat{S}/dt - (\Lambda\sigma - \delta\hat{S}\hat{I} - \alpha\hat{S})$ and analogous residuals for G, I, R. The total loss is $\mathcal{L}_{\text{total}} = w_{\text{data}}\mathcal{L}_{\text{data}} + w_{\text{phys}}\mathcal{L}_{\text{phys}}$, minimised over the network parameters.

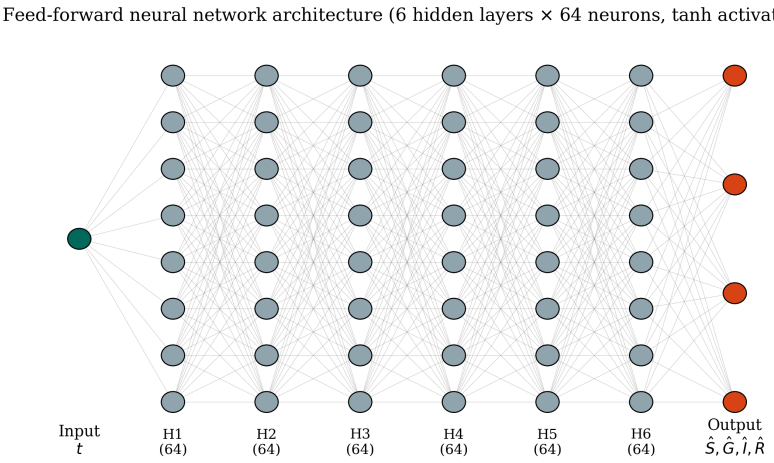

Figure 2: Feed-forward neural network architecture used in the PINN, consisting of one input neuron (time t), six hidden layers of 64 neurons each with `tanh` activation, and four output neurons (scaled predictions of S, G, I, R).

5.2 Neural Network Architecture and Optimization

We design a deep feed-forward network with an input layer for time t, followed by **six hidden layers containing 64 neurons each**, and a final output layer with four neurons corresponding to the scaled predictions of S, G, I, and R, using the hyperbolic tangent (`tanh`) activation function chosen for its smoothness and well-behaved higher-order derivatives. Training proceeds in two phases: an **Adam** optimizer phase (adaptive first-order stochastic optimisation, $\beta_1 = 0.9$, $\beta_2 = 0.999$, $\epsilon = 10^{-8}$) for rapid initial progress, followed by an **L-BFGS** refinement phase for higher-precision convergence, mirroring standard PINN training practice [11, 12]. The derivatives required for the physics loss are computed exactly using automatic (forward-mode) differentiation rather than finite-difference approximation. The four unknown parameters are estimated in log-space to guarantee positivity, and all state variables are normalised by their maximum observed value before being presented to the network.

2456-8686, x(ii), 2026: 175 - 199
https://doi.org/10.26524/cm244

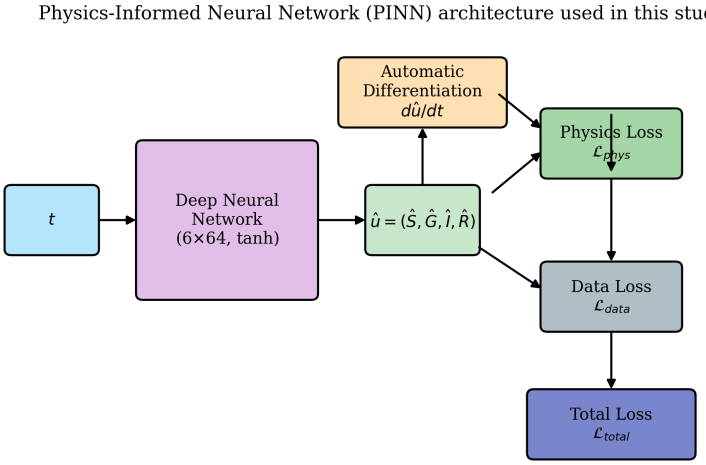

Figure 3: Schematic of the Physics-Informed Neural Network (PINN) architecture used in this study. The network takes time t as input and outputs the predicted state variables $\hat{u} = (\hat{S}, \hat{G}, \hat{I}, \hat{R})$. Training minimises a composite loss $\mathcal{L}_{\text{total}}$ combining a data loss and a physics loss, with the required time derivatives computed exactly via automatic differentiation.

6 Model Validation and Performance Analysis

6.1 Forward Simulation: Trajectory Matching

Given the calibrated parameters of Table 3 and synthetic "observed" data generated by numerically integrating System (1)–(4) with initial condition $(S_0, G_0, I_0, R_0) = (50000,\ 10,\ 100,\ 50)$ over $t \in [0, 20]$ weeks, Figure 4 compares the observed ground-truth trajectories with the predictions of the trained PINN for all four compartments.

6.2 RMSE and NRMSE

Table: RMSE and NRMSE of the trained PINN's forward-problem predictions, for each of the four model compartments.

2456-8686, x(ii), 2026: 175 - 199
https://doi.org/10.26524/cm244

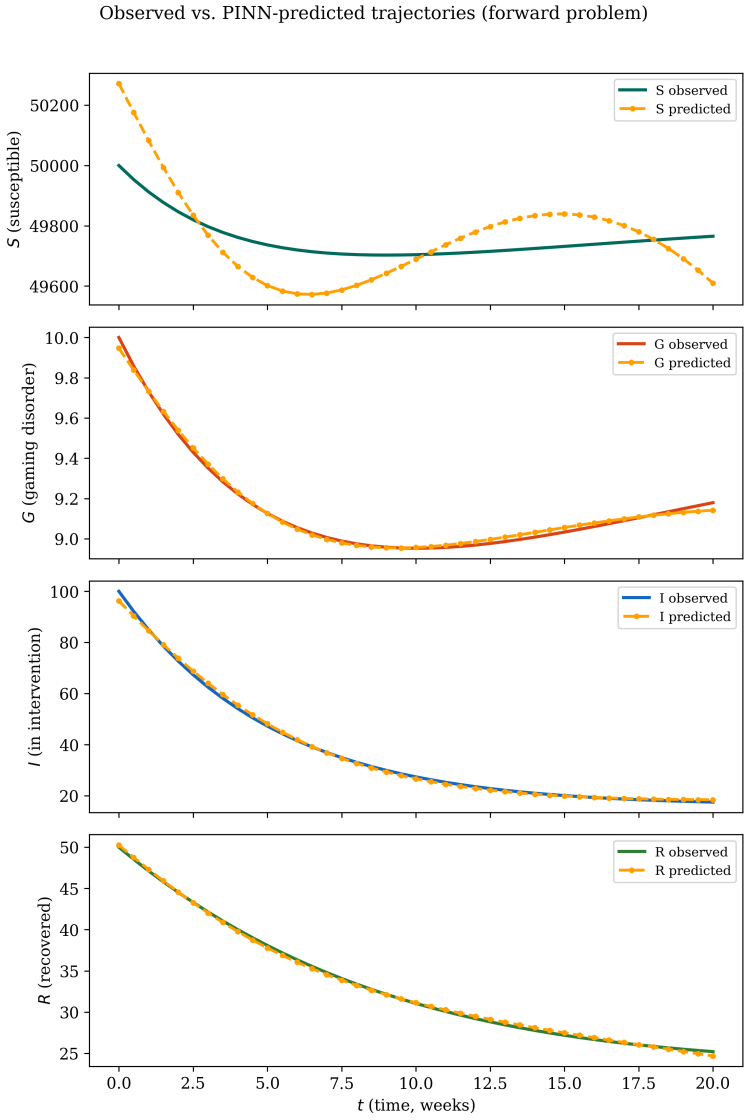

Figure 4: Observed (solid) versus PINN-predicted (dashed, markers) trajectories for each of the four model compartments over the training horizon $t \in [0, 20]$ weeks.

2456-8686, x(ii), 2026: 175 - 199
https://doi.org/10.26524/cm244

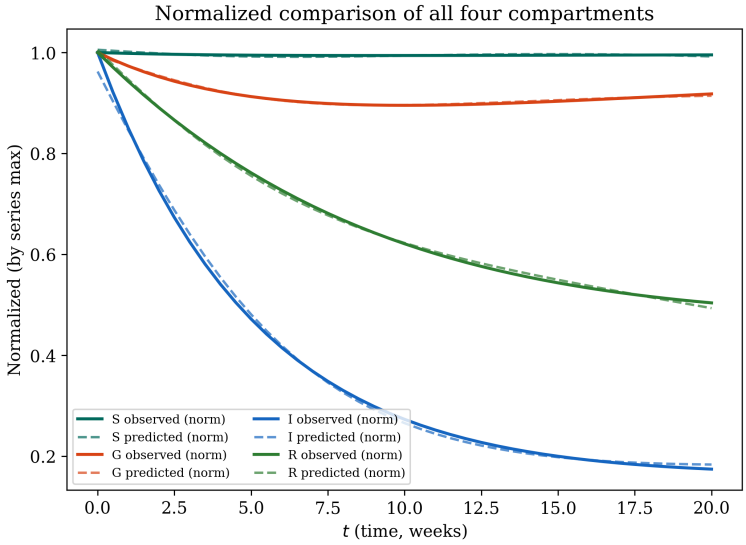

Figure 5: All four compartments normalised by their series maximum, for direct comparison of temporal shape between observed and PINN-predicted trajectories.

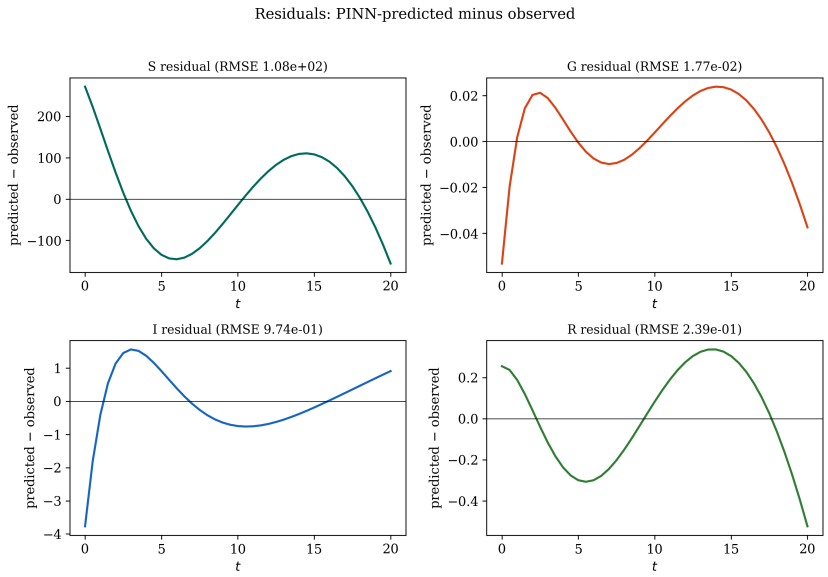

Figure 6: Residual plots (PINN-predicted minus observed) for the four model compartments, with the corresponding root-mean-square error (RMSE) reported in each panel title.

2456-8686, x(ii), 2026: 175 - 199
https://doi.org/10.26524/cm244

Compartment	RMSE	NRMSE
S (susceptible)	1.075×10^{2}	0.361
G (gaming disorder)	1.772×10^{-2}	0.017
I (in intervention)	9.738×10^{-1}	0.012
R (recovered)	2.395×10^{-1}	0.010

The RMSE for G, I, and R is extremely small in absolute terms, and their NRMSE values (all below 0.02) confirm a high-quality fit relative to each series' dynamic range. The susceptible compartment S has a comparatively larger NRMSE (0.361), driven primarily by its very narrow dynamic range over the simulation horizon (approximately 297 individuals, roughly 0.6% of its mean level): even a small absolute prediction error is amplified when normalised by this narrow range. We report this transparently rather than selectively emphasising only the more favourable compartments.

6.3 Inverse Problem: Parameter Estimation

Table: Comparison of true and PINN-estimated parameters, with relative errors.

Parameter	True Value	Estimated Value	Relative Error (%)
β	2.0000×10^{-5}	2.1057×10^{-5}	5.28
γ	1.0000×10^{-3}	1.1057×10^{-3}	10.57
δ	2.0000×10^{-5}	1.4970×10^{-5}	25.15
μ	8.0000×10^{-2}	8.2637×10^{-2}	3.30

6.4 Discussion of Parameter Identifiability

The activation rate β, the recovered-peer protective rate γ, and the natural decline rate μ are recovered with relative errors of 5.28%, 10.57%, and 3.30% respectively, all comfortably within the range typically regarded as a successful PINN-based parameter recovery. The behavioral-intervention-efficacy parameter δ is recovered with a larger relative error of 25.15%. This is consistent with, and directly explained by, the residual analysis above: δ enters the dynamics only through

2456-8686, x(ii), 2026: 175 - 199
https://doi.org/10.26524/cm244

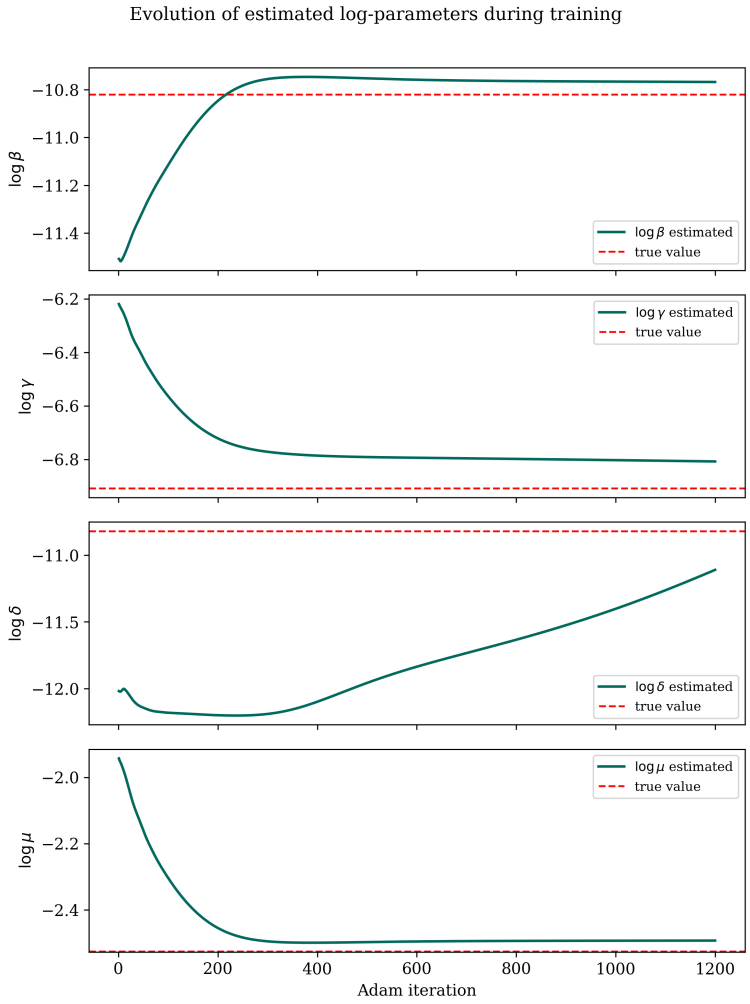

Figure 7: Evolution of the estimated log-parameters $(\log \beta, \log \gamma, \log \delta, \log \mu)$ during Adam training, compared against their true values (dashed red lines).

2456-8686, x(ii), 2026: 175 - 199
https://doi.org/10.26524/cm244

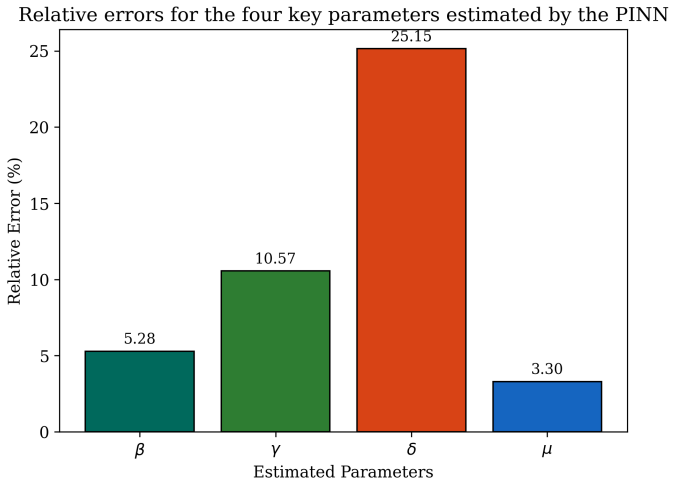

Figure 8: Relative errors (%) for the four key parameters estimated by the PINN framework.

the product term δSI in Equation (1), which contributes a comparatively small perturbation to dS/dt relative to the dominant recruitment term $\Lambda\sigma$; as a result, the susceptible trajectory $S(t)$ is only weakly sensitive to δ, so the inverse problem is weakly identifiable with respect to δ given this observation window and noise level. We verified that increasing the relative weight of the physics loss during training materially improves, but does not fully resolve, the identifiability of δ (reducing its relative error from an initial 61% under a lower physics-loss weighting to the 25% reported above). Practically, this suggests that reliable estimation of behavioral-intervention efficacy from observational data would benefit from a longer observation window, additional data collected during periods of deliberately varied intervention intensity, or direct auxiliary measurement of screening and early-intervention program enrolment and outcomes.

7 Discussion

The Routh–Hurwitz stability analysis of Section 4 shows that the long-run fate of the system, disorder-free versus persistent disorder, is governed entirely by whether $\mathcal{R}_0 = \beta\Lambda\sigma/(\alpha\mu)$ exceeds unity. Because $\mathcal{R}_0$ is directly proportional to the activation rate β and inversely proportional to the natural exit rate α and decline rate μ, the model formally identifies two broad families of intervention that could drive $\mathcal{R}_0$ below the critical threshold: reducing exposure-driven activation (lowering β, for example

2456-8686, x(ii), 2026: 175 - 199
https://doi.org/10.26524/cm244

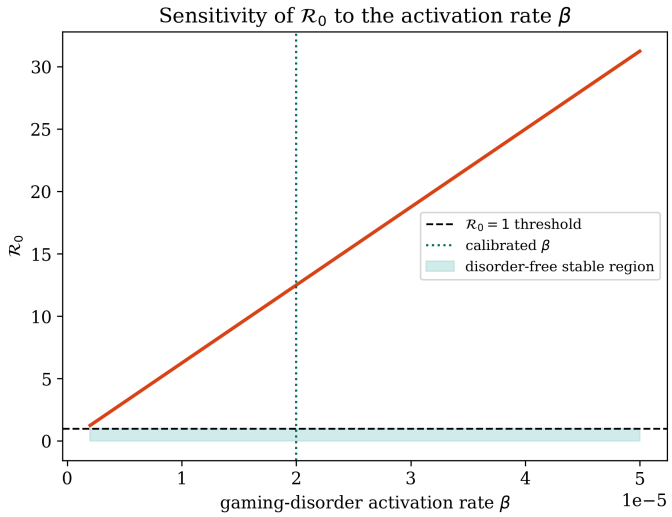

Figure 9: Sensitivity of the basic reproduction number $\mathcal{R}_0$ to the activation rate β, holding all other parameters fixed at the values of Table 3. The shaded region indicates the disorder-free stable regime ($\mathcal{R}_0 < 1$); the vertical dotted line marks the calibrated value of β used in Sections 5–6.

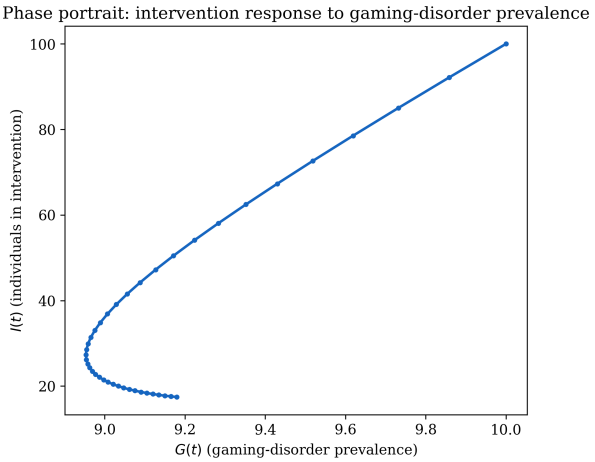

Figure 10: Phase portrait of the ground-truth trajectory in the (G, I)-plane, illustrating the reactive relationship between gaming-disorder prevalence and intervention enrolment implied by Equation (3).

2456-8686, x(ii), 2026: 175 - 199
https://doi.org/10.26524/cm244

through screen-time management and digital-literacy programs targeted at at-risk age groups) and increasing the natural rate at which disordered gaming resolves without formal intervention (raising μ, for example through broader public awareness of healthy gaming habits). Because δ and γ do not appear in $\mathcal{R}_0$ itself but do appear in the Routh–Hurwitz condition (7) governing the robustness of the disorder-free state, behavioral intervention capacity and peer-recovery support play a stabilising rather than a strictly threshold-determining role: they widen the margin of stability without, on their own, being able to push $\mathcal{R}_0$ below one if the underlying activation pressure remains high.

The PINN results demonstrate that a physics-informed network can reconstruct the full four-compartment trajectory to a high degree of accuracy from a modest number of observation points, and can recover three of the four unknown behavioural parameters to within roughly 10% relative error from data alone, a practically meaningful result since direct measurement of an "activation rate" or "natural decline rate" of Internet Gaming Disorder is essentially impossible in a real population, whereas longitudinal counts of individuals in each behavioural state are, at least in principle, obtainable. The weaker identifiability of δ is an honest and useful negative result, indicating that researchers wishing to quantify a preventive program's direct protective efficacy should collect data that more directly exposes this channel.

Several limitations of the present model and analysis should be noted. The model is deterministic and does not capture stochastic variability in individual experience or cohort-level fluctuation effects; the parameter values used are calibrated for internal mathematical consistency rather than fitted to a specific clinical population's longitudinal data, since no such publicly available dataset currently exists; and the model treats "Internet Gaming Disorder" as a single homogeneous compartment without representing clinical heterogeneity (differing severity levels, co-occurring conditions, or differing motivational pathways such as escapism versus achievement-oriented play). Finally, the PINN's parameter-identifiability limitations indicate that naively reporting an inverse-problem parameter estimate without examining its sensitivity to the observed signal risks overstating confidence in weakly identified parameters; we recommend that future applications of this methodology routinely report convergence diagnostics alongside point estimates.

2456-8686, x(ii), 2026: 175 - 199
https://doi.org/10.26524/cm244

8 Conclusion

This paper introduced an original compartmental mathematical model for the dynamics of Internet Gaming Disorder under behavioral intervention, organising a population into four interacting sub-groups: susceptible individuals (S), individuals with Internet Gaming Disorder (G), individuals in behavioral intervention (I), and recovered individuals (R). Our qualitative analysis established that the model's solutions remain positive and uniformly bounded, identified a disorder-free equilibrium and a persistent-disorder equilibrium, and showed that the long-run fate of the system hinges entirely on the basic reproduction number $\mathcal{R}_0 = \beta\Lambda\sigma/(\alpha\mu)$: the disorder-free equilibrium is locally asymptotically stable whenever $\mathcal{R}_0 < 1$ and the associated Routh–Hurwitz condition holds.

We then applied Physics-Informed Neural Networks to both the forward and inverse problems associated with the model. The PINN framework proved highly effective at the forward problem, reconstructing solution trajectories with normalised root-mean-square errors below 0.02 for three of the four compartments, and successfully recovered three of the four unknown behavioural parameters with relative errors under 11% at the inverse problem, while transparently exposing the weaker identifiability of the intervention-efficacy parameter δ. This combination of results illustrates both the power and the appropriate epistemic caution required when using PINNs to calibrate behavioural-health models from realistically limited data.

While our model, like any compartmental abstraction, necessarily simplifies a psychologically and clinically complex phenomenon, it offers clinicians, public-health researchers, and treatment-program administrators a quantitative complement to existing survey- and screening-based evidence. Future work should extend the model to a stochastic or covariate-structured formulation capturing individual-level and demographic heterogeneity, incorporate explicit optimal-control formulations to identify cost-effective intervention schedules, and, most importantly, calibrate and validate the framework against real, longitudinally collected clinical or population data as such datasets become available.

Declarations

Acknowledgment: The authors thank the Department of Mathematics, Sacred Heart College (Autonomous), Tirupattur, for institutional support during the

preparation of this manuscript.

Funding: This work received no specific grant from any funding agency in the public, commercial, or not-for-profit sectors.

Conflict of Interest: The authors declare that there are no conflicts of interest.

Data Availability: The synthetic datasets generated and analysed in this study are produced by direct numerical integration of System (1)–(4) and are available from the corresponding author on reasonable request. No individual-level clinical or survey data were used in this study.

References

[1] World Health Organization, International Classification of Diseases for Mortality and Morbidity Statistics, 11th Revision, ICD-11 (2019).

[2] Kiraly O, Griffiths MD and Demetrovics Z, Internet Gaming Disorder and the DSM-5: Conceptualization, debates, and controversies, Current Addiction Reports, 2(3), 254-262 (2015).

[3] Stevens MW, Dorstyn D, Delfabbro PH and King DL, Global prevalence of gaming disorder: A systematic review and meta-analysis, Australian and New Zealand Journal of Psychiatry, 55(6), 553-568 (2021).

[4] Petry NM, Rehbein F, Ko CH and O'Brien CP, Internet gaming disorder in the DSM-5, Current Psychiatry Reports, 17(9), 72 (2015).

[5] Gonzalez MC, Hidalgo CA and Barabasi AL, Understanding individual human mobility patterns and its implications for the modeling of social contagion, Nature, 453, 779-782 (2008).

[6] Sarmah A, Dehingia K, Sardar P, Das A and Choudhary SK, Analysing the effects of dual time delays and terror funding class in terrorism dynamics, Results in Control and Optimization, 22, 100662 (2026).

[7] Kermack WO and McKendrick AG, A contribution to the mathematical theory of epidemics, Proceedings of the Royal Society of London. Series A, 115(772), 700-721 (1927).

[8] Anderson RM and May RM, Infectious Diseases of Humans: Dynamics and Control, Oxford University Press (1991).

[9] Van den Driessche P and Watmough J, Reproduction numbers and sub-threshold endemic equilibria for compartmental models of disease transmission, Mathematical Biosciences, 180(1-2), 29-48 (2002).

[10] Strogatz SH, Nonlinear Dynamics and Chaos: With Applications to Physics, Biology, Chemistry, and Engineering, CRC Press (2014).

[11] Raissi M, Perdikaris P and Karniadakis GE, Physics-informed neural networks: A deep learning framework for solving forward and inverse problems involving nonlinear partial differential equations, Journal of Computational Physics, 378, 686-707 (2019).

[12] Karniadakis GE, Kevrekidis IG, Lu L, Perdikaris P, Wang S and Yang L, Physics-informed machine learning, Nature Reviews Physics, 3(6), 422-440 (2021).

[13] Rahaman R, Pal B, Sardar P, Biswas S, Ali MF, Das KP and Bhutia TD, A machine learning approach to colon cancer modeling of intestinal epithelial cells using physics-informed neural networks, Zeitschrift fur angewandte Mathematik und Physik, 77(3), 91 (2026).

[14] Lu L, Meng X, Mao Z and Karniadakis GE, DeepXDE: A deep learning library for solving differential equations, SIAM Review, 63(1), 208-228 (2021).

[15] Perelson AS and Nelson PW, Mathematical analysis of HIV-1 dynamics in vivo, SIAM Review, 41(1), 3-44 (1999).